IOPscience iopscience.iop.org

Home Search Collections Journals About Contact us My IOPscience

Polaronic effects on lithium motion in intercalated perovskite lithium lanthanum titanate observed by ^{7}Li NMR and impedance spectroscopy

This article has been downloaded from IOPscience. Please scroll down to see the full text article.

1999 J. Phys.: Condens. Matter 11 10401

(http://iopscience.iop.org/0953-8984/11/50/330)

View the table of contents for this issue, or go to the journal homepage for more

Download details:
IP Address: 171.66.16.218
The article was downloaded on 15/05/2010 at 19:15

Please note that terms and conditions apply.

J. Phys.: Condens. Matter **11** (1999) 10401–10417. Printed in the UK PII: S0953-8984(99)04589-0

Polaronic effects on lithium motion in intercalated perovskite lithium lanthanum titanate observed by ^{7}Li NMR and impedance spectroscopy

J Emery†‖, O Bohnke‡, J L Fourquet‡, J Y Buzaré†, P Florian§ and D Massiot§

† Laboratoire de Physique de la Matière Condensée (UPRESA 6087 CNRS), Université du Maine, Avenue O Messiaen, 72085 Le Mans Cédex 9, France
‡ Laboratoire des Fluorures (UPRESA 6010 CNRS), Université du Maine, Avenue O Messiaen, 72085 Le Mans Cédex 9, France
§ Centre de Recherche sur les Matériaux à Haute Température, CNRS, 45071 Orléans Cedex 2, France

E-mail: joel.emery@univ-lemans.fr

Received 26 May 1999

Abstract. The long-range and short-range motion of lithium ions into an electrochemically intercalated $Li_{3x}La_{2/3-x}TiO_3$ (LLTO) sintered pellet has been studied by ac impedance spectroscopy and ^{7}Li solid state nuclear magnetic resonance (NMR). The temperature dependence of the dc conductivity and the intercalation ratio dependence of the chemical shift, the relative intensity of the resonance line, the spin–lattice and the spin–spin relaxation times of ^{7}Li NMR experiments are indicative of polaron formation at the initial stage of intercalation. The total dc conductivity measured in the temperature range 45–600 K and the shape of the impedance diagrams show that after intercalation the conductivity is both ionic and electronic in nature. However for temperatures lower than 300 K the total conductivity is mainly dominated by the electronic one and for temperatures higher than 400 K the total conductivity is dominated by the ionic one. Moreover at low temperatures, when electronic conductivity dominates, the temperature dependence of the conductivity agrees well with a polaron model for conduction in these intercalated oxides.

The NMR experiments clearly show that the resonance peak decreases strongly as intercalation occurs. This is explained by a coupling between the electronic and the Li^+ nuclear spins leading to an unobservability of some Li^+ nuclei in NMR. The other Li^+ nuclei, which do not interact directly with the electronic spins, are responsible for the observed NMR signal. If the static effect of the intercalation is weak and leads to a very small chemical shift variation, variable temperature ^{7}Li NMR spin–lattice and spin–spin relaxation measurements show that the presence of electrons acts essentially on the dynamics of the Li^+ nuclei through the lattice modification induced by the polaron formation. At the beginning of the intercalation the inverse of the relaxation time T_1 of the observed Li^+ nuclei decreases by one order of magnitude. At the same time the linewidth of the resonance peak ($\propto 1/T_2$) decreases abruptly. The motion of the lithium ions is sharply enhanced. For further intercalation, $1/T_1$ decreases and the linewidth of the central peak increases indicating that the variations of the relaxation times are mostly governed by the variations of the spectral densities of the Li^+ motion. Consequently, the lithium motion decreases gradually as intercalation proceeds. These results are in good agreement with a lattice modification due to polaron formation during intercalation.

1. Introduction

The compounds belonging to the solid solution $(La_{2/3-x}Li_{3x}\square_{1/3-2x})TiO_3$ present a perovskite-type structure ABO_3 with cation deficiency ($\square$) at the A sites. Previous studies

‖ Corresponding author.

0953-8984/99/5010401+17$30.00 © 1999 IOP Publishing Ltd

have shown that a pure phase solid solution exists only in the domain $0.04 < x < 0.14$ [1]. The presence of these A-site vacancies is favourable for high mobility of lithium ions. A maximum ionic conductivity of 8×10^{-4} S cm^{-1} has been found at room temperature for the composition $x = 0.08$ after sintering [2]. However despite this high conductivity, the presence of Ti^{4+} ions in the structure and the possible reduction of this ion with Li metal (or any other material which has an oxido-reduction potential smaller than that of the couple Ti^{4+}/Ti^{3+}, i.e. 1.5 V/Li) limits the choice of the electrodes and then the use of this material as an electrolyte for a high voltage battery. In this paper we investigated another property of this oxide, the intercalation of Li^+ ions in the structure. Previous studies have shown indeed that lithium ions can be reversibly inserted into this oxide and that its diffusion coefficient is very high (of the order of 10^{-8} cm^2 s^{-1}) [2, 3]. As far as we know, this is one of the highest diffusion coefficients observed in a lithium inserted oxide.

In this work, the ^{7}Li NMR technique and impedance spectroscopy have been used in a large temperature range in order to investigate both the short-range and long-range dynamics in the intercalated $(La_{0.59}Li_{0.24+dx}\square_{0.17-dx})(Ti^{3+}_{dx}Ti^{4+}_{1-dx}O_3)$ compound, with dx the intercalation ratio. This material has been obtained by electrochemical intercalation of Li^+ ions and electrons into $(La_{2/3-x}Li_{3x}\square_{1/3-2x})TiO_3$ of $x = 0.080$ composition. Comparison will be made with the non-inserted material that we previously studied [4, 5]. The motivation of this work is to modify the interactions between the Li^+ ions and their environment by the introduction of ions and electrons into the host matrix and to understand how these interactions influence both the relaxation of ^{7}Li ions and the conductivity.

2. Experimental

2.1. Sample preparation

$Li_{3x}La_{2/3-x}TiO_3$ (LLTO) was prepared from stoichiometric amounts of Li_2CO_3, TiO_2 and La_2O_3 (high purity grade) by solid state reaction [2]. The obtained powder was then ground, pressed into pellets of 5 mm of diameter and 1–2 mm of thickness under a pressure of 250 MPa and then sintered at 1300 °C for 6 h at a sweep rate of 5 °C min^{-1}. Since an Li_2O loss occurs during the sintering process, chemical analysis of Li^+ was performed by flame emission technique in order to determine the exact composition of the sintered compound. The present study has been carried out with the $Li_{3x}La_{2/3-x}TiO_3$ ($x = 0.080 \pm 0.003$) compound. The crystal structure and ionic conductivity were verified by x-ray diffraction (XRD) and impedance spectroscopy. They were in perfect accordance with the results previously published [1, 2].

Intercalation of lithium into LLTO was performed by galvanostatic discharge using the 1287 Solartron electrochemical interface. A lithium reference electrode and lithium counter-electrode were used in a three-electrode cell. The working electrode was a 5 mm diameter pellet of the sintered oxide. No mixture of LLTO with graphite and binder but only the monolithic pellet was used to exclude any side reactions during intercalation and any side interactions in ^{7}Li NMR. $LiClO_4$ (0.1 M) dissolved in anhydrous propylene carbonate was used as electrolyte. The cell was mounted in an argon filled dry box to prevent any oxygen or water contaminations. The pellet was pressed with silver paste onto a Pt current collector to ensure good electronic contact. The mass of the pellet was of the order of 140 mg. The applied cathodic current was 5 μA at the beginning of the intercalation to ensure a slow kinetics and to allow the lithium to diffuse into the bulk of the pellet. After one day of intercalation the current was increased to 10 or 20 μA until the desired intercalation ratio (dx) was reached. During the intercalation the potential of the electrode was continuously checked to prevent any Li plating which could react with the residual water contained in the electrolyte and consequently lead to a wrong

calculated dx value. Four samples with dx = 0.010, 0.030, 0.064 and 0.108 ($\pm$0.003) have been prepared. The intercalation was accompanied by a colour change from pale yellow to dark blue in the whole pellet.

2.2. Conductivity measurements

Conductivity measurements were carried out by the complex impedance method with a frequency response analyser 1276 (Solartron) from 40 to 600 K in the frequency range 5 MHz–100 Hz with 30 measurements per decade and an applied voltage of 20 mV (r.m.s.). (It was found that the response of the electrochemical system remains linear from 5 to 1000 mV.) Gold was sputtered on both sides of the pellet as ionically blocking electrodes. For measurements above room temperature (RT) the sample was fixed up in a two-electrode cell in an oven under pure dehydrated N_2 atmosphere. For measurements below RT the sample was fixed up in a two-electrode cell under vacuum in a cryogenerator. The sample was allowed to equilibrate for 1 to 2 h before measurement until obtaining reproducible impedance spectra. The Zview equivalent circuit software of Solartron has been used to fit the impedance spectra to the equivalent circuit described in this paper.

2.3. ^{7}Li NMR measurements

Static ^{7}Li NMR spectra were recorded at a frequency of 116.6 MHz. As previously described [5] a Bruker MSL300 spectrometer was used for temperature between 150 and 410 K and a Bruker ADX300 spectrometer for higher temperatures. For chemical shift determination a saturated LiCl solution was used as an external reference. This solution was also used to set up the radiofrequency power: the $\pi/2$ liquid pulse time was 5 μs which corresponds to a radiofrequency amplitude of $\nu_1 = 50$ kHz and a non-selective regime. The ^{7}Li chemical shift of the central line was determined by using the WINFIT NMR software [6]. In this study ^{7}Li spectra were recorded with a simple sequence $\pi/2$-acquisition, while the spin–lattice relaxation times T_1 were obtained by using an inversion recovery sequence (π–τ–$\pi/2$ acquisition) in the temperature range 150–900 K. It is worth noticing that the recovery magnetization shows a monoexponential behaviour. T_1 values have been obtained at each temperature by fitting the experimental magnetization to the following exponential function:

$$M(\tau) = M_0[1 - 2\alpha \exp(-\tau/T_1)] \tag{1}$$

where the spin–lattice relaxation time T_1, the thermal equilibrium magnetization M_0 and α were considered to be adjustable parameters in a least-squares fitting procedure. The value of α has been found to be very close to 1. It can be noticed that the saturation experiments to determine T_1 gave the same results as the inversion recovery experiments (in the former case α is found to be very close to 0.5). Particular attention has been paid to the spectral window used in the experiments in order to observe new resonance peaks. This window was typically of the order of 50 to 500 kHz.

For experiments below RT, a ZrO_2 crucible was filled with the powdered sample in the argon dry box before introduction into the spectrometer. For high temperature experiments, the sample was put in a high purity boron nitride crucible (grade AX05, carborundum) and an argon flow was used to avoid any reoxidation of the intercalated oxide. In order to verify that the sample does not undergo reoxidation during the experiments, we performed an RT acquisition before and after the experiments. The spectra were perfectly identical.

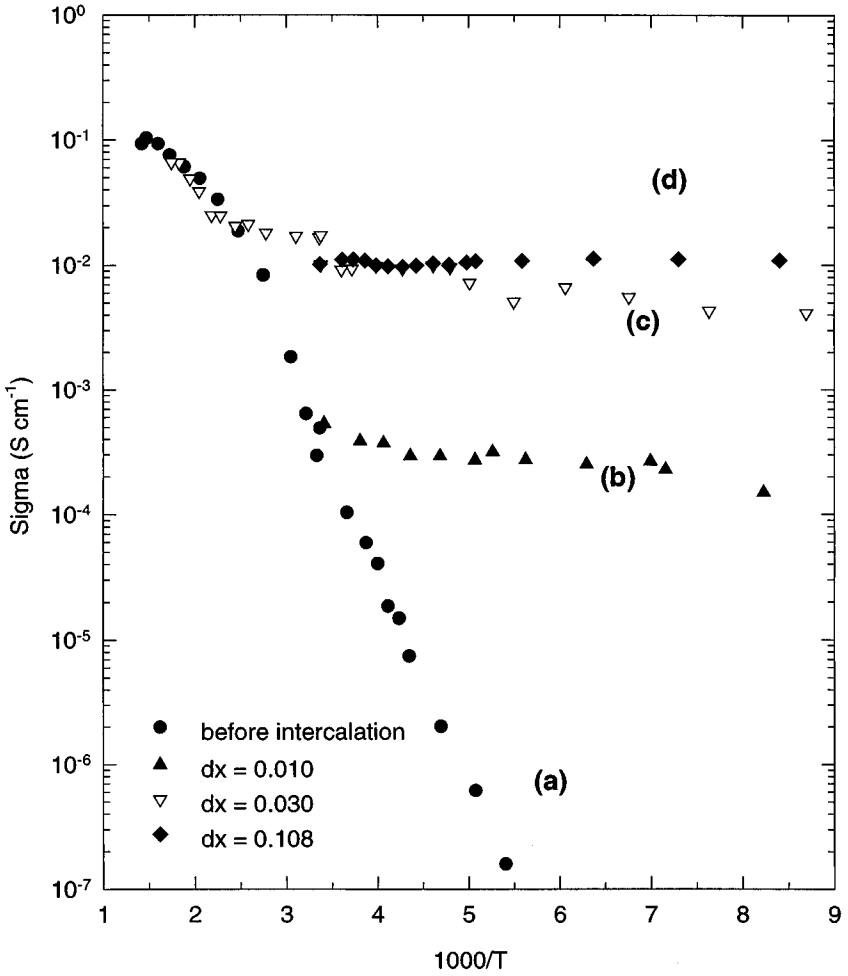

Figure 1. Total dc conductivity as a function of reciprocal temperature of $(La_{2/3-x}Li_{3x})TiO_3$ ($x = 0.080$) before (a) and after electrochemical intercalation (b to d) of lithium ions.

3. Results

3.1. Conductivity

Figure 1 presents the total dc conductivity of LLTO as a function of reciprocal temperature before intercalation (curve a) and after injection of both Li^+ and electrons into the oxide matrix (curves b to d). These data have been obtained in the temperature range 100–600 K. The total conductivity increases as intercalation increases. For example at 200 K the dc conductivity is around 10^{-6} S cm^{-1} before intercalation and increases by three orders of magnitude for $dx = 0.01$ to reach finally a value of 10^{-2} S cm^{-1} for $dx = 0.108$. This increase means that the injected electrons are delocalized as generally observed in intercalated transition metal oxides. As previously shown, the conductivity of LLTO before intercalation is purely ionic with an activation energy of 0.36 eV [2]. After intercalation the conductivity is both ionic and electronic in nature and mainly dominated by the electronic conductivity at low temperatures ($T < 300$ K). At higher temperatures ($T > 300$ K) the ionic conductivity of the intercalated

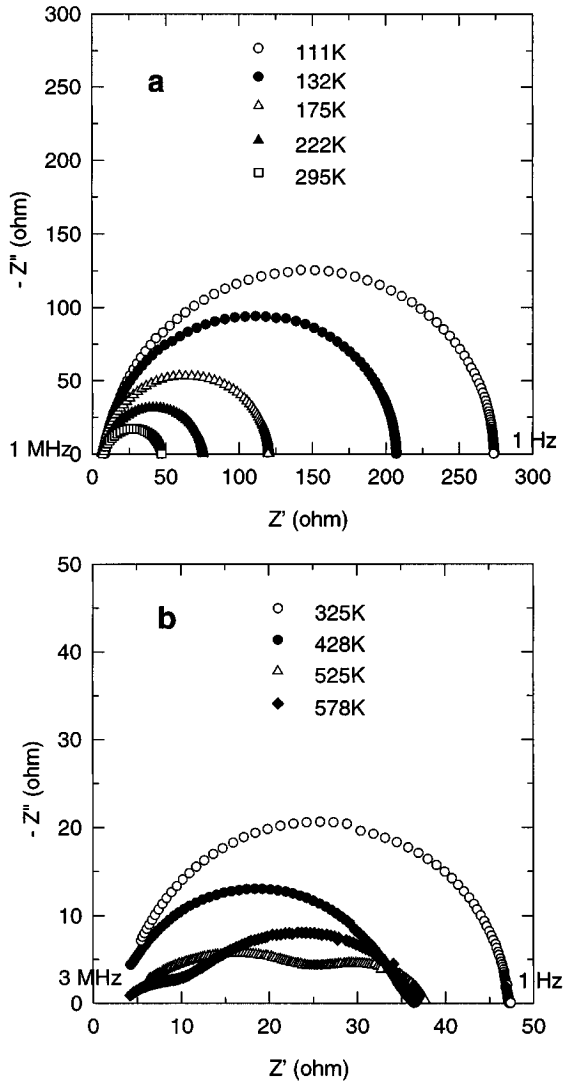

Figure 2. Nyquist plots of the intercalated $(La_{0.59}Li_{0.24+dx})(Ti^{3+}_{dx}Ti^{4+}_{1-dx}O_3)$ oxide with $dx = 0.020$ at different temperatures: below (a) and above room temperature (b).

oxides becomes of the same order of magnitude as the electronic one and even greater for $T > 400$ K. At these temperatures the total conductivity is then dominated by the ionic one and the conductivity behaviour of the intercalated material follows the non-intercalated one, as shown in figure 1 (curve c for $dx = 0.030$).

The presence of two conduction pathways (electronic and ionic) is also observed in the Nyquist impedance diagrams shown in figure 2 for $dx = 0.020$. The impedance diagrams change with temperature. At low temperatures ($T < 300$ K, figure 2(a)), the diagrams exhibit only one semi-circle ascribed to the electronic pathway. At higher temperatures (figure 2(b)), the diagrams display two semi-circles whose characteristics change with temperature.

Figure 3 presents the variation of the dc conductivity as a function of reciprocal temperature in the low temperature domain, i.e. 300–45 K, for $dx = 0.020$. The most striking characteristics

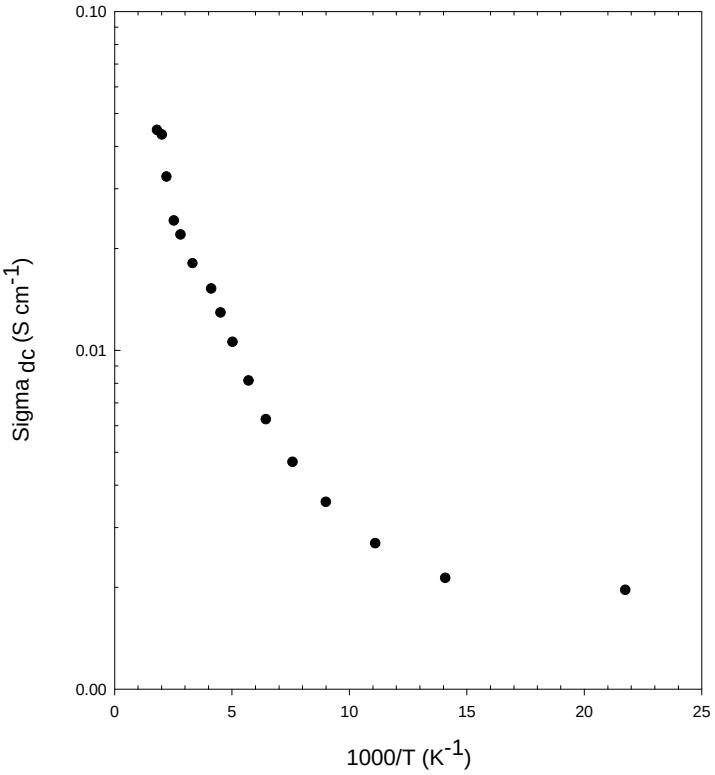

Figure 3. The dc conductivity as a function of reciprocal temperature for the intercalated $(La_{0.59}Li_{0.24+dx})(Ti^{3+}_{dx}Ti^{4+}_{1-dx}O_3)$ oxide with d$x = 0.020$.

of these intercalated oxides are observed at low temperatures where the conductivity is predominantly electronic in nature. The activation energy for dc conduction is found to be temperature dependent and saturation occurs at very low temperatures ($T < 70$ K).

3.2. ^{7}Li NMR

Figure 4 shows non-normalized static NMR spectra of ^{7}Li ($I = 3/2$) obtained at room temperature by using a phase cycling single pulse sequence ($\pi/2$-acquisition). The spectral window shown in this figure is not very large for clarity. It is important to mention that no other peak is present in the spectra when a large spectral window is used. Spectrum (a) which is related to the non-intercalated ($x = 0.080$) compound is given as reference. All the other spectra (from b to e) are relative to the intercalated materials obtained from the same initial compound ($x = 0.080$). The intercalation increases from spectrum b (d$x = 0.010$) to c (d$x = 0.030$) to d (d$x = 0.064$) and finally to spectrum e (d$x = 0.108$). These spectra are dominated by a narrow peak coming from the $-1/2 \leftrightarrow 1/2$ transition. The satellite transitions ($\pm 3/2 \leftrightarrow \pm 1/2$), which appear between 100 and 200 ppm and which are not shown in figure 4, are less resolvable in the intercalated materials than in the non-intercalated one. We had previously shown, by static ^{7}Li NMR and ^{7}Li MAS, that on the non-intercalated oxide, the satellite transitions, associated with electric quadrupolar interactions, exist but are not very well resolved [4]. It had been suggested that this effect might be due to the

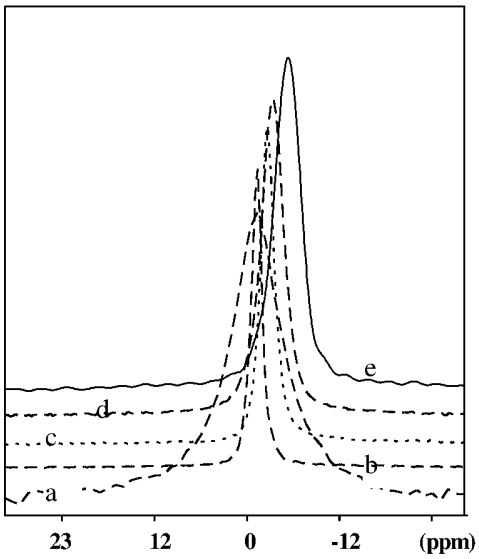

Figure 4. Static ^{7}Li NMR spectra recorded at 116.6 MHz and at room temperature for $(La_{2/3-x}Li_{3x})TiO_3$ ($x = 0.080$) before (a) and after intercalation (b: d$x = 0.010$, c: d$x = 0.030$, d: d$x = 0.060$, e: d$x = 0.108$).

existence of Li^+ ions with different environments leading to a distribution of each energy levels. This is in good agreement with the crystallographic structure of the oxide which presents a random distribution of Li^+ and La^{3+} ions [1]. This distribution acts at first order of perturbation on the satellite transitions and at second order of perturbation on the central transition. Consequently, this central transition is enhanced when the satellite ones spread over a large frequency range. On the other hand, the motion of the Li^+ ions, in an intermediate regime, may also lead to a broadening of the satellites. In both cases (different environments of the Li^+ ions and/or dynamics of these Li^+ ions), these contributions to the shape of the spectra lead to a better resolution of the satellites as temperature increases, as shown in a previous paper [5]. For intercalated materials, the satellites are less and less resolvable as intercalation proceeds, suggesting either that the distribution of the quadrupolar splittings is even greater or that the dipolar and quadrupolar interactions that broaden these satellites are more important.

Figure 5 shows the evolution of both the chemical shift (a) and the relative intensity of the central line (b) as intercalation proceeds. It can be observed that the resonance peak intensity decreases sharply as intercalation occurs. Figure 6 shows the variation of the inverse of the spin–lattice relaxation time as a function of reciprocal temperature before and after intercalation. We can separate the intercalation in two steps: a first one at the beginning of the intercalation (corresponding to the intercalation of the first electrons and ions into the oxide) and a second one when intercalation proceeds. At the onset of the intercalation, four effects can easily be observed in figures 4, 5 and 6: a strong decrease of the relative intensity of the resonance peak and a small chemical shift towards negative value (figure 5), a sudden and important decrease of the linewidth of the resonance peak (figure 4), and finally a decrease of one order of magnitude of $1/T_1$ (figure 6). Then as intercalation proceeds, on one hand the relative intensity of the central peak as well as the chemical shift and the $1/T_1$ continue to decrease continuously; on the other hand the width of the resonance peak increases. It can be also observed that the maximum of the $1/T_1$–$1000/T$ curve does not significantly vary with intercalation (the maximum shifts slightly towards high temperatures).

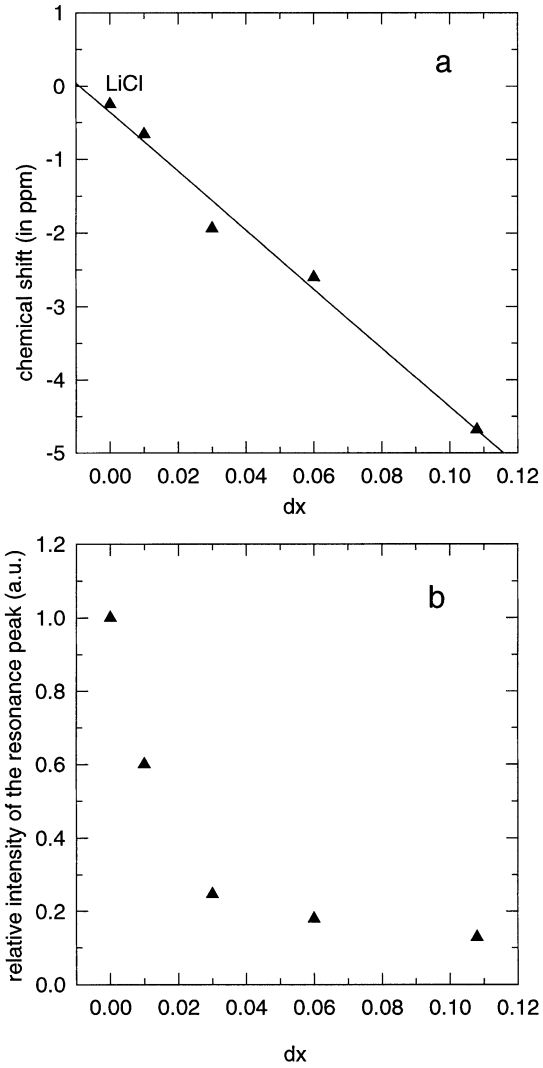

Figure 5. Variation of the chemical shift (a) and of the relative intensity of the ^{7}Li resonance peak (b) as a function of the intercalation parameter dx.

4. Discussion

It is well known that the intercalation mechanism involves the injection of both ions and electrons into the host matrix. To balance the negative charge brought by the electrons, Li^+ ions coming from the electrolyte are also intercalated in (or near) the vacant A sites of the perovskite structure. Since it has been proved on other transition metal oxides (i.e. WO_3 [7, 8]) that the intercalated lithium ions enter the oxide without its solvatation shell, the intercalated lithium ions cannot be different from the lithium ions present in the structure before electrochemical reaction. Moreover the size of the bottleneck the lithium ions have to pass through to go to (or near) the A site is too small to allow a solvated ion to enter the material. We can then postulate that a distinction between different lithium ions, i.e. those present in the structure before intercalation and the intercalated ions coming from the electrolyte, is not reasonable.

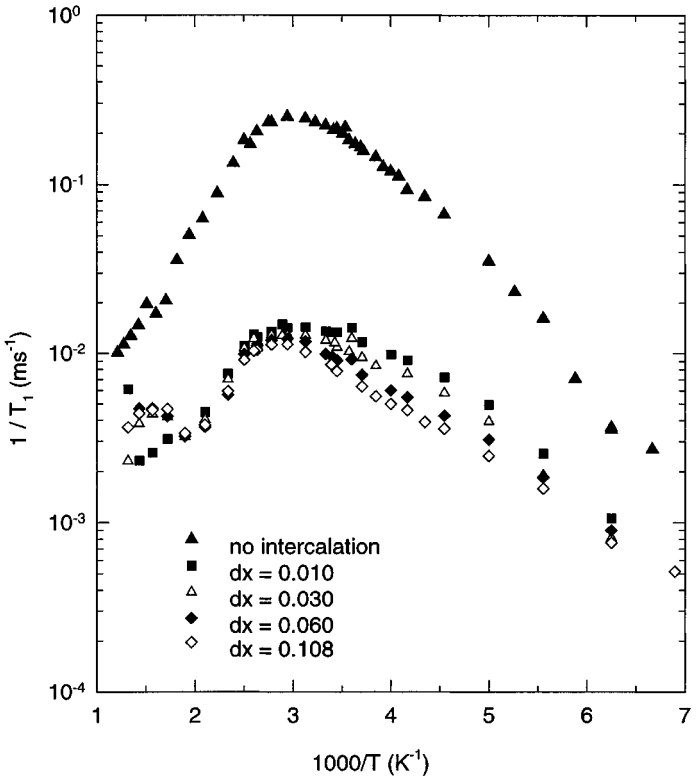

Figure 6. Logarithmic plots of the inverse of the spin–lattice relaxation time $1/T_1$ as a function of the reciprocal temperature for $(La_{2/3-x}Li_{3x})TiO_3$ ($x = 0.080$) before and after intercalation.

The intercalation phenomenon in metal transition oxides (WO_3, MoO_3, TiO_2) is accompanied by both an enhancement of the conductivity and the blue colouration of the intercalated material. This phenomenon has been extensively studied and used for electrochromic applications [9]. Optical-absorption measurements performed on these intercalated metal transition oxides lead to evidence of polaron formation [10]. Polarons are created when electrons polarize their surroundings leading to localized states with a finite mobility. The materials exhibit polaron absorption in the near infrared, which makes the oxides bluish. In our materials, the injected electrons are transferred to the Ti^{4+} ions leading to the formation of some Ti^{3+} ions. The local polarization of the surroundings of the Ti^{4+} ions leads to a deformation around these ions. Because of coulombic repulsions the electronic cloud of the oxygen ions tends to be pushed towards the A sites of the structure. The electronic density around the Li^+ environment then increases slightly leading to the observed shift of the resonance peak towards lower frequencies. This shift of the oxygen electronic cloud toward the Li^+ site modifies the Li^+ environment leading to an Li^+ motion change and to a T_1 variation. The experimental results suggest then the existence of polarons in these intercalated oxides.

4.1. Conductivity

The low frequency semi-circle, which appears at high temperatures (figure 2(b)), can be ascribed to the impedance of the ionic pathway and the high frequency one to the impedance of

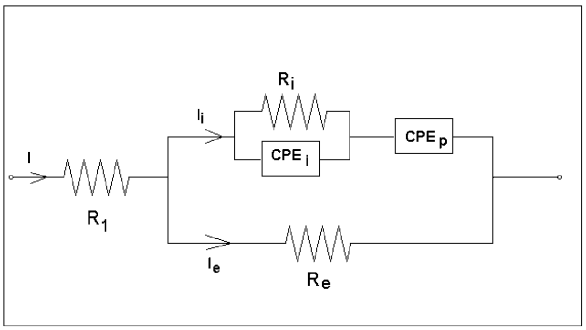

Figure 7. Equivalent circuit used to model the complex impedance data of figure 2.

the electronic pathway. This behaviour is described by the electrical model shown in figure 7. The current (I) induced in the sample under the ac applied voltage is due to both the electron (I_e) and the ion (I_i) motions. The ionic pathway is electrically described by a resistance (R_i) in parallel with a capacitance or a constant phase element (CPE_i) which describes the polarization of the dielectric medium through which the ions have to move. Moreover in the ionic pathway another CPE (CPE_p) describes the polarization of the electrodes at low frequency due to the ionic motion. The electronic pathway is described by a resistance (R_e). The resistance R_1 refers to the resistance of the sputtered gold electrodes; it is very small and lies between 2 and 4 ohms for all the samples. At low temperatures $R_i \gg R_e$ and the electrical circuit is made of the resistance of the electronic pathway in parallel with the capacitance of the bulk oxide. This gives rise to a semi-circle as shown in figure 2(a). When temperature increases, R_i decreases and the full circuit of figure 7 has to be taken into account. A small polarization appears at the electrodes and the polarization capacitance increases as the ionic motion is enhanced. The impedance diagrams display two semi-circles as shown in figure 2(b). Figure 8 presents the fitting of four impedance diagrams obtained on the intercalated sample of figure 2 ($\mathrm{d}x = 0.020$) at four different temperatures with the values of the fitted parameters obtained according to the electrical model of figure 7. The resistance R_e decreases as temperature increases suggesting that at this intercalation ratio the material does not have a metallic behaviour. The resistance R_i decreases as temperature increases and the capacitance CPE_i increases with temperature. As expected the capacitance of the intercalated oxide ($\approx 10^{-8}$ F) is higher than the capacitance of the bulk oxide before intercalation ($\approx 10^{-11}$ F). This means that the dielectric properties of the oxide changes with intercalation. The polarization capacitance CPE_p increases as temperature increases since the ionic motion is thermally activated and more and more ions are blocked at the electrode interface during one alternance of the ac voltage.

Figure 3 shows that the variation of the dc conductivity, from room temperature to 45 K, decreases by one order of magnitude, that the conductivity data follow a smooth variation and that saturation occurs at low temperature ($T < 70$ K). This temperature dependence of conductivity agrees well with a polaron model for conduction in these intercalated oxides. The polaron model predicts that an appreciable departure from a linear $\ln \sigma$–$1/T$ plot should occur below a given temperature [11]. The total conductivity is then the sum of the hopping (thermally activated motion) and the tunnelling contributions. The tunnelling contribution to conductivity dominates only at low temperatures (below 70 K) leading to the saturation effect. Above 155 K the hopping process is dominant with an activation energy of 0.05 eV. Between 155 and 70 K an intermediate regime in the polaron conductivity appears.

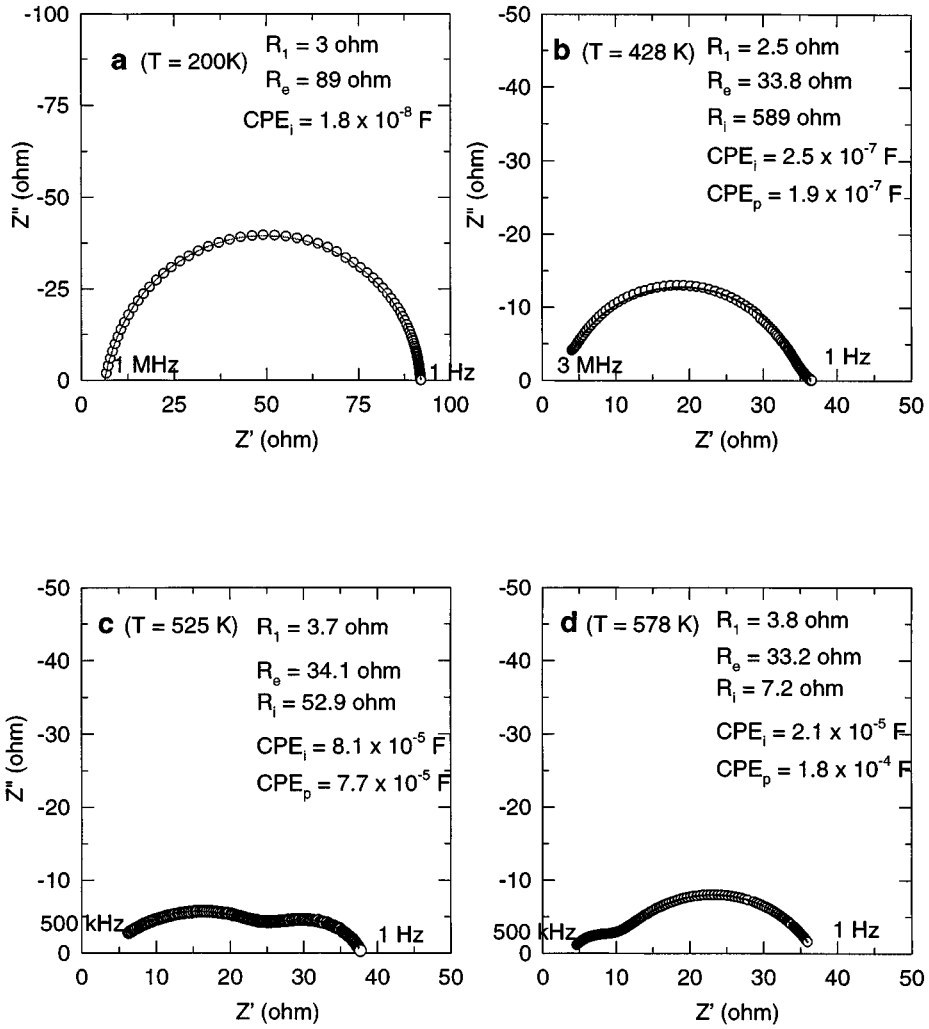

Figure 8. Nyquist plots of the intercalated $(La_{0.59}Li_{0.24+dx})(Ti^{3+}_{dx}Ti^{4+}_{1-dx}O_3)$ oxide with $dx = 0.020$ at four temperatures. The experimental data are shown by the circles. The lines show the fitted impedance plots obtained from the equivalent circuit of figure 7 and fitted with the Zview software. At each temperature, the electrical parameters obtained from the fitting procedure are given in the figures.

4.2. ^{7}Li NMR

As shown in conductivity experiments the intercalation modifies the dielectric properties of the material. This is also observed through the increase of the pulse time T_{90} which varies from 7.4 μs in the non-intercalated compound to 14 μs in the intercalated one for $dx = 0.108$, for example.

Before analysing the NMR results we need to understand the strong decrease of the relative intensity of the resonance line occurring after intercalation, as shown in figure 5. This result does not agree with the presence of more lithium ions in the intercalated oxide (the presence of electrons and consequently of more lithium ions is clearly indicated by the blue colour of the samples after intercalation). So, it suggests the presence of a new and strong coupling

leading to the presence of ^{7}Li nuclei which become unobservable in NMR. On the one hand, recently the formation of Li^+–Li^+ ion pairs in solid lithium conductors has been suggested by Sigaryov *et al* [12, 13]. The existence of such pairs would lead to a particular shape of the spectra corresponding to the coupling between the two nuclear spins, but not to a decrease of the signal intensity as experimentally observed. This assumption can then be ruled out. On the other, a coupling between the spins of the injected electrons and some Li^+ nuclei may lead to a strong modification of the NMR spectra either through static mechanisms (modification of the chemical shift, quadrupolar tensor) or through dynamical ones (relaxation times). Since no new resonance peak is observed and since the observed resonance line is not strongly modified in both shape and position, this implies that the decrease of the signal intensity arises from a decrease of the number of observed Li^+ ions. The presence of a strong interaction between some Li^+ nuclei and the injected electronic spins may lead to a resonance frequency out of the NMR range or/and a very fast relaxation (an Overhauser effect experiment could confirm the existence of interaction between electronic and nuclear spins [14, 15]). Consequently, the NMR signal observed in our experiments is due to the ^{7}Li nuclei which do not interact directly with the electronic spins; the other ^{7}Li nuclei, which undergo a strong interaction with these latter spins, become unobservable. This phenomenon has also been observed by other authors during deintercalation of lithium from $LiCoO_2$ [16].

In the following, we are then concerned with the resonance line observed in NMR and then with the Li^+ nuclei which do not interact strongly with the electronic spins. In this discussion, we have to distinguish between the static and the dynamic effects of the intercalation process. The static contribution is mainly shown by the variation of the chemical shift although the dynamic one is shown by the variations of the Li^+ relaxation times (T_1 and T_2). It is important to notice that this latter contribution involves the spectral densities of the lattice fluctuations.

Figure 5 shows a static effect of the intercalation. This process shifts the resonance peak by some ppm to lower frequencies from that for Li^+ in solution (LiCl). This result cannot be compared to the shift of 240 ppm for Li in Li metal [17]. It indicates that the electronic density in the Li^+ ion environment increases as intercalation occurs. However the small deviation values of this chemical shift indicate also: (i) that the injected electrons are not localized on the lithium ions, (ii) that these ions remain in the same ionized state during the intercalation. This is in good agreement with thermodynamic study on the intercalated oxides which could not agree with a reduction of Li^+ ions (this latter reduction occurs around 0 V/Li) but rather with the reduction of Ti^{4+} ions during electrochemical intercalation (experimentally, this reduction occurs at a voltage of 1.5 V/Li [2]).

If the static effect of the intercalation is weak (no direct coupling), as shown above, the electron injection into the host matrix leads to dynamic effects which are more important than the static one. These dynamic effects are mainly observed in figures 6 and 4 in which the $1/T_1$ and the $1/T_2$ relaxation time behaviours are presented respectively. Figure 6 shows that $1/T_1$ sharply decreases by one order of magnitude as intercalation occurs and continuously decreases with further intercalation. The decrease of $1/T_1$ indicates that the observed ^{7}Li nuclei do not undergo new interactions with the injected electron spins. Indeed, the observed T_1 combines different spin–lattice relaxation mechanisms such as dipole–dipole (T_{1_d}), quadrupolar (T_{1_q}) and chemical shift ($T_{1_{cs}}$) mechanisms. As intercalation occurs, electrons are injected into the oxide and we could expect that another relaxation mechanism takes place and contributes to a change in the T_1 value. Since all these contributions combine in reciprocal fashion, i.e. the overall relaxation rate being the sum of the relaxation rates attributed to individual mechanisms, the observed $1/T_1$ can be written as

$$\frac{1}{T_1} = \frac{1}{T_{1_d}} + \frac{1}{T_{1_q}} + \frac{1}{T_{1_{cs}}} + \frac{1}{T_{1_{ne}}} \tag{2}$$

where $T_{1_{ne}}$ is the spin–lattice relaxation time of the interaction between the Li^+ nuclei and the injected electrons. According to this relationship the addition of interactions would lead to an increase of the $1/T_1$ value. This is not experimentally observed and this result means that the observed ^{7}Li nuclei do not interact directly and significantly with the injected electrons. This result agrees also with the small observed chemical shift variations.

The decrease of the NMR signal which does not agree with the number of injected electrons, as shown in figure 5, proves that the electrons move on several Ti^{4+} ions. Moreover the presence of ^{7}Li nuclei which do not interact directly with the injected electrons indicates that the electrons are not totally delocalized on all the Ti^{4+} ions. This result can be explained by the fact that all the Ti ions in the structure are not energetically equivalent owing to structural disorder in the La^{3+} ion distribution and then to the presence of different next-nearest neighbours [1].

The presence of electrons acts then essentially on the dynamics (T_1 and T_2) of the observed Li^+ nuclei through the lattice modification since the NMR observed ^{7}Li nuclei do not interact directly with the electronic spins. These results confirm the presence of polarons after intercalation, as previously shown by the temperature dependence of the dc conductivity (figure 3). The experimental data presented in figures 6 and 4 show two different behaviours of the relaxation times according to the intercalation step considered: (i) at the beginning of the intercalation both $1/T_1$ (figure 6) and $1/T_2$ (proportional to the linewidth of the resonance peak, figure 4 spectrum b) decrease, (ii) for further intercalation, these two relaxation times vary in opposite directions; $1/T_1$ continues to decrease (figure 6) although $1/T_2$ increases (figure 4 spectra c to e).

From a general point of view, the relaxation times T_1 and T_2 vary with both the interactions involved in the mechanism of relaxation through the C_i constants and the correlation functions of the Li^+ motion through the spectral densities $J_{\alpha\beta}(\omega)$, according to the following well known relationships:

$$\frac{1}{T_{1,i}} = C_i[J_{21}(\omega_0) + 4J_{22}(2\omega_0)] \tag{3}$$

$$\frac{1}{T_{2,i}} = C_i[3J_{20}(0) + 5J_{21}(\omega_0) + 2J_{22}(2\omega_0)] \tag{4}$$

where ω_0 is the Larmor frequency. C_i are constants which account for the interaction involved in the mechanism of relaxation (i stands for the different above mentioned interactions: d, q, cs, ne), $J_{\alpha\beta}(\omega)$ is the spectral density of the motion measured at ω frequency and associated with the irreducible tensor operator $T_{\alpha\beta}$ in which the Hamiltonians of all the interactions are developed [18]. We have to recall that C_i depend on the spin states only and $J_{\alpha\beta}(\omega)$ on the lattice only. Therefore these two contributions to the variations of $1/T_1$ and $1/T_2$ can be differentiated.

It is important to remark that the main difference between relationships (3) and (4) comes from the static term $J_{20}(0)$. Consequently, opposite variations of $1/T_1$ and $1/T_2$ can occur only through a strong variation of this static term ($\omega = 0$). In other words, if at the beginning of the intercalation it is not possible to differentiate between the contribution of the interactions and the contribution of the spectral densities to the relaxation time variations since $1/T_1$ and $1/T_2$ vary in the same direction, it is possible to determine the most important contributions during further intercalation since the relaxation times vary then in opposite directions. Therefore the increase of $1/T_2$ as intercalation proceeds can be explained by a great increase of $J_{20}(0)$ able to compensate the decrease of $J_{21}(\omega_0)$ and $J_{22}(2\omega_0)$ responsible for the decrease of $1/T_1$. This result clearly shows that the correlation functions of the motion of the observed Li^+ nuclei and

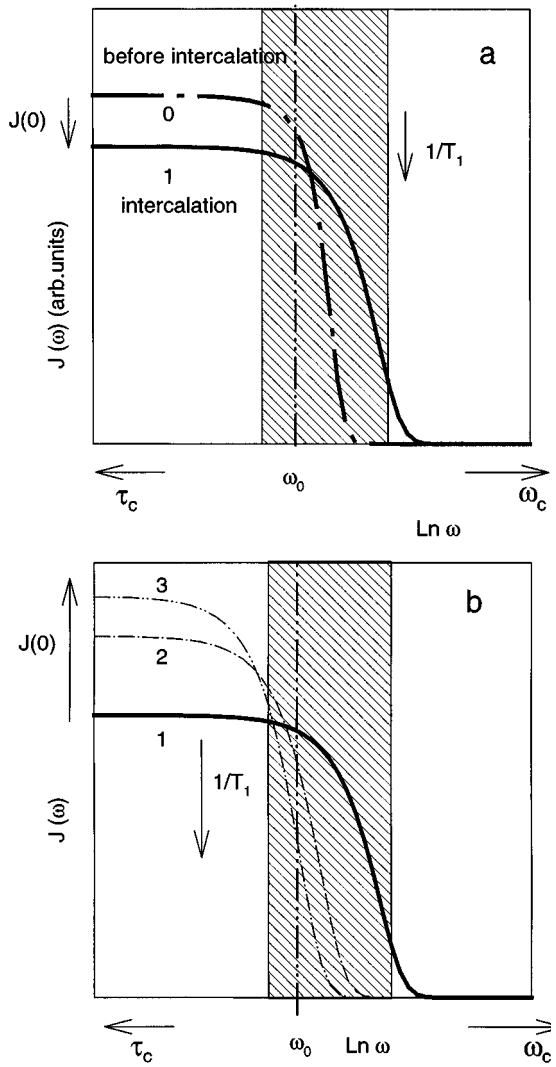

Figure 9. Schematic representation of the variation of the motional spectral density as a function of intercalation: (a) evolution of $J(\omega)$ before intercalation (curve 0) and at the beginning of the intercalation (curve 1); (b) shows the evolution of $J(\omega)$ as intercalation proceeds from curves 1 to 3. ω_0 represents the Larmor frequency and the dashed region shows the characteristic frequency range of the fluctuations.

then the spectral densities $J_{\alpha\beta}(\omega)$ undergo a sudden change through the lattice deformation as polarons are formed in the host matrix.

It is now possible to schematically describe the variations of the spectral densities as a function of intercalation. This is presented in figure 9(a) for the beginning of the intercalation and (b) for further intercalation. It has to be noticed that the observation of the maximum of $1/T_1$ around room temperature means that the Larmor frequency is close to the characteristic frequency of the fluctuations that cause the relaxation (dashed range in figure 9). Consequently we are very sensitive to any variation of the spectral density. This maximum does not significantly vary from $\mathrm{d}x = 0$ to $\mathrm{d}x = 0.108$. As suggested by the above discussion and the

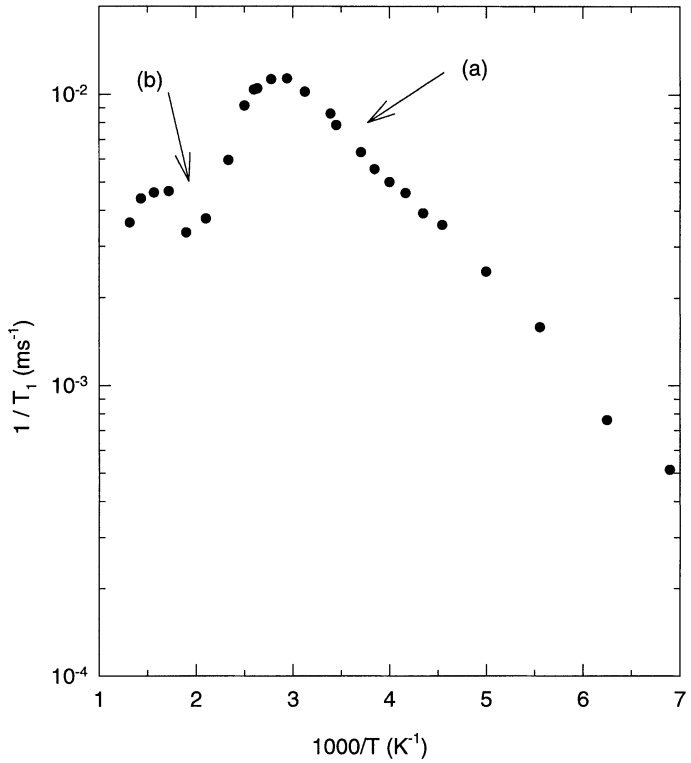

Figure 10. Logarithmic plots of the reciprocal of the spin–lattice relaxation time $1/T_1$ as a function of the reciprocal temperature for the intercalated $(La_{0.59}Li_{0.24+dx})(Ti^{3+}_{dx}Ti^{4+}_{1-dx}O_3)$ oxide with $dx = 0.108$. The arrows indicate the two features occurring in the curve.

relationships (3) and (4), the sharp decrease of both $1/T_1$ and $1/T_2$ at the beginning of the intercalation is linked to a decrease of the spectral densities. This implies that the characteristic correlation time, τ_c, decreases according to the schema (a) of figure 9. As intercalation proceeds, the linewidth slightly increases, then $J(0)$ increases to compensate the decrease of $J_{21}(\omega_0)$ and $J_{22}(2\omega_0)$. Consequently the characteristic time τ_c increases again as shown in schema (b) of figure 9. The intercalation leads then to an enhancement of the lithium motion at the beginning of the reaction followed by the slowing down of this motion as intercalation proceeds. This enhancement can be explained by the formation of polarons in the host matrix which change suddenly the surrounding lattice of the Li^+ ions and act on the random motion of these ions (electron thermal motion induced by polaron random motion). Thereafter, as lithium ions enter the material, the A sites are more and more occupied, decreasing the mobility of the lithium ions and leading to a slowing down of the random motion. This is in good agreement with lithium hops occurring through the vacant A sites.

Finally, two particular features are observed in figure 10 as intercalation becomes important ($dx = 0.108$). The first one (a) appears for $3 < 1000/T < 4$ and the second one (b) at $1000/T \approx 2$. The first one is typical of the presence of two mechanisms of relaxation which are also suggested in the non-intercalated samples shown in figure 6 [4, 5]. We can observe that the intercalation amplifies the difference between these two contributions. The second feature, which has not been observed in the non-intercalated sample, suggests an instability in the intercalated compound which becomes more important when intercalation proceeds.

This behaviour is reversible as observed by NMR. We think that the low temperature feature, which is enhanced in the intercalated compounds, is implied in the conduction mechanism of LLTO; this assumption needs more investigation.

5. Conclusion

The results obtained by ^{7}Li NMR clearly show that during intercalation some of the ^{7}Li nuclear spins undergo a direct interaction with the injected electronic spins leading to a strong decrease of the NMR signal owing to some ^{7}Li nuclei becoming NMR silent. Nevertheless the NMR signal does not completely disappear. The observed resonance peak is due to the ^{7}Li nuclei which do not interact directly with the electronic spins. The presence of such nuclei suggests that the injected electrons are not totally delocalized on all the Ti^{4+} ions. The variation of the relaxation times T_1 and T_2 of these observed nuclei clearly reveal a modification of the Li^+ ion environment during intercalation. This modification is explained by the formation of polarons. This assumption is also confirmed by the temperature dependence of the dc conductivity. The static as well as the dynamic effects of the intercalation are observed in NMR. The static effect is mostly observed by the chemical shift parameter that deviates towards negative values. This small increase of the electronic density is due to the presence of the injected electrons on the Ti^{4+} ions which displace the electronic cloud of the oxide ions towards the Li^+ sites. The small variation of the chemical shift also shows that the Li^+ nuclei and the electronic spins do not directly interact. However an indirect interaction through the lattice deformation induced by the injected electrons and giving rise to a polaron can explain the experimental results. The dynamic effects experimentally shown by the T_1 behaviour agree with this analysis since T_1 increases as intercalation occurs, showing that no other mechanism can be involved in the spin–lattice relaxation. Moreover the variations of T_1 and T_2 in the opposite directions with further intercalation have to be attributed to a change in the motional spectral densities. Finally, two relaxation mechanisms are observed which are better separated in the presence of polarons. Ac impedance spectroscopy shows clearly the presence of two conductive pathways for the ions and the electrons respectively. The electronic conductivity is predominant in the conductivity process at low temperatures, the ionic one becoming more and more important when temperature increases. This study is a step in the understanding of the mechanisms involved in the ionic conduction process in this kind of material.

References

[1] Fourquet J L, Duroy H and Crosnier-Lopez M P 1996 *J. Solid State Chem.* **127** 283
[2] Bohnke O, Bohnke C and Fourquet J L 1996 *Solid State Ion.* **91** 21
[3] Birke P, Scharner S, Huggins R A and Weppner W 1997 *J. Electrochem. Soc.* **144** L167
[4] Emery J, Buzaré J Y, Bohnke O and Fourquet J L 1997 *Solid State Ion.* **99** 41
[5] Bohnke O, Emery J, Veron A, Fourquet J L, Buzaré J Y, Florian P and Massiot D 1998 *Solid State Ion.* **109** 25
[6] Massiot D, Thiele H and Germanius A 1994 *Bruker Rep.* **43** 140
[7] Bohnke O, Vuillemin B, Gabrielli C, Keddam M, Perrot H, Takenouti H and Toressi R 1995 *Electrochim. Acta* **17** 2755
[8] Bohnke O, Vuillemin B, Gabrielli C, Keddam M, Perrot H, Takenouti H and Toressi R 1995 *Electrochim. Acta* **17** 2765
[9] Bohnke O 1992 *Proton Conductors—Chemistry of Solid State Materials 2* ed P Colomban (Cambridge: Cambridge University Press) p 551
[10] Granqvist C G 1997 *Solid State Electrochemistry* ed P J Gellings and H J M Bouwmeester (New York: Chemical Rubber Company) pp 587–615
[11] Austin I G and Mott N F 1969 *Adv. Phys.* **18** 41
[12] Pronin I S, Vashman A A and Sigaryov S E 1993 *Phys. Rev.* B **48** 16 463

[13] Vashman A A, Pronin I S and Sigaryov S E 1992 *Solid State Ion.* **58** 201
[14] Overhauser A W 1959 *Phys. Rev.* **92** 411
[15] Abragam A, Combrisson J and Salomon I 1958 *C. R. Acad. Sci., Paris* **246** 1035
[16] Imanishi N, Fujiyoshi M, Takeda Y, Yamamoto O and Tabuchi M 1999 *Solid State Ion.* **118** 121
[17] McKinnon W R 1987 *Chemical Physics of Intercalation (NATO ASI B)* vol B172, ed A P Legrand and S Flanfrois (New York: Plenum) p 181
[18] Mehring M 1983 *Principles of High Resolution NMR in Solids* (Berlin: Springer)